ADVANCED FUNCTIONAL MATERIALS
www.afm-journal.de

Polythiophenes for High-Performance N-type Organic Electrochemical Transistors

Chan Zhang, Yuting Zheng, Yanru Li, Zhongyuan Xue, Xiuyuan Zhu, Jiawei Chen, Jianeng Ma, Zhi Zhang, Hongliang Zhong, Wan Yue, Ting Lei,* and Zhuping Fei**

N-type organic electrochemical transistor (OECT) materials play a critical role in building low-power complementary circuits and advanced biosensors. However, current n-type OECT materials are usually based on complicated fused aromatics and cannot simultaneously achieve high performance and good stability. Despite a few design strategies for n-type polythiophene-based organic field-effect transistor (OFET) materials, they cannot be directly applied to OECT materials which work in highly doped states. Here, it is reported that polythiophenes, which always show p-type OECT behaviors, can be designed and converted to high-performance n-type OECT materials by a synergy of introducing electron-withdrawing (EW) groups, controlling polaron delocalization, and tuning molecular packing. Two isomeric n-type polythiophene derivatives, *o*-CNgTVT-2FT and *i*-CNgTVT-2FT are designed, which show interesting and distinct OECT properties. *o*-CNgTVT-2FT exhibits excellent n-type OECT performance with a remarkable figure of merit (μC^*) of 100.0 F cm^{-1} V^{-1} s^{-1} while keeping an outstanding current retention of 93.6% after 1000 switching cycles in the air. The high performance can be largely attributed to its more delocalized and stabilized negative charges, efficient 3D charge transport channels, and favorable film morphology. The work highlights that without complex fused aromatic rings, carefully designed polythiophene polymers can also be used for high-performance and stable n-type OECTs.

1. Introduction

Over the last decade, organic electrochemical transistors (OECTs) have attracted widespread attention due to their low operating voltage (<0.8 V), low power consumption, high transconductance, and good biocompatibility,[1–4] exhibiting promising potentials in biosensors,[5–7] bioelectronics,[8–10] and neuromorphic computing.[11–13] Conjugated polymers, which can efficiently transport ions and electrons, are ideal channel materials for OECTs.[14–17] Despite significant progress in p-type polymer OECT materials, achieving a figure of merit (μC^*) exceeding 300 F cm^{-1} V^{-1} s^{-1} with good operational stability,[18–20] n-type OECT materials have lagged far behind. To meet the growing demand for low-power complementary OECT circuits and high-sensitive sensors,[21–26] it is imperative to develop high-performance and stable n-type OECT materials. So far, many efforts have been devoted to designing n-type OECT materials based on different complex electron-deficient fused aromatic building blocks (**Figure 1a**), such as diketopyrrolopyrrole (e.g., P(gTDPP2FT)),[27] isoindigo (e.g., gAIID-2FT),[28] naphthalenediimide (e.g., p(gNDI-gT2)),[21] BDOPV (e.g., p(C-T))[29] and bithiophene diimide (e.g., f-BTI2TEG-FT),[30] as well as ladder-type polymers (e.g., BBL,[24,31] PgNaN).[32] Nevertheless, these materials showed either low μC^* or poor stability compared to their p-type counterparts,[29,33–40] with only a few polymers achieving μC^* over 50 F cm^{-1} V^{-1} s^{-1} (Table S1,

C. Zhang, Y. Li, J. Chen, J. Ma, Z. Fei
Institute of Molecular Plus
Department of Chemistry
Key Laboratory of Organic Integrated Circuits
Ministry of Education
Tianjin University
Tianjin 300072, P. R. China
E-mail: zfei@tju.edu.cn

Y. Zheng, Z. Zhang, T. Lei
Key Laboratory of Polymer Chemistry and Physics of Ministry of Education
School of Materials Science and Engineering
Peking University
Beijing 100871, P. R. China
E-mail: zhizhang@pku.edu.cn; tinglei@pku.edu.cn

The ORCID identification number(s) for the author(s) of this article can be found under https://doi.org/10.1002/adfm.202419706

Y. Li, Z. Fei
Haihe Laboratory of Sustainable Chemical Transformations
Tianjin 300192, P. R. China

Z. Xue, H. Zhong
School of Chemistry and Chemical Engineering
Shanghai Key Lab of Electrical Insulation and Thermal Aging
Shanghai Jiao Tong University
Shanghai 200240, P. R. China

X. Zhu, W. Yue
School of Materials Science and Engineering
Sun Yat-Sen University
Guangzhou 510275, P. R. China

DOI: 10.1002/adfm.202419706

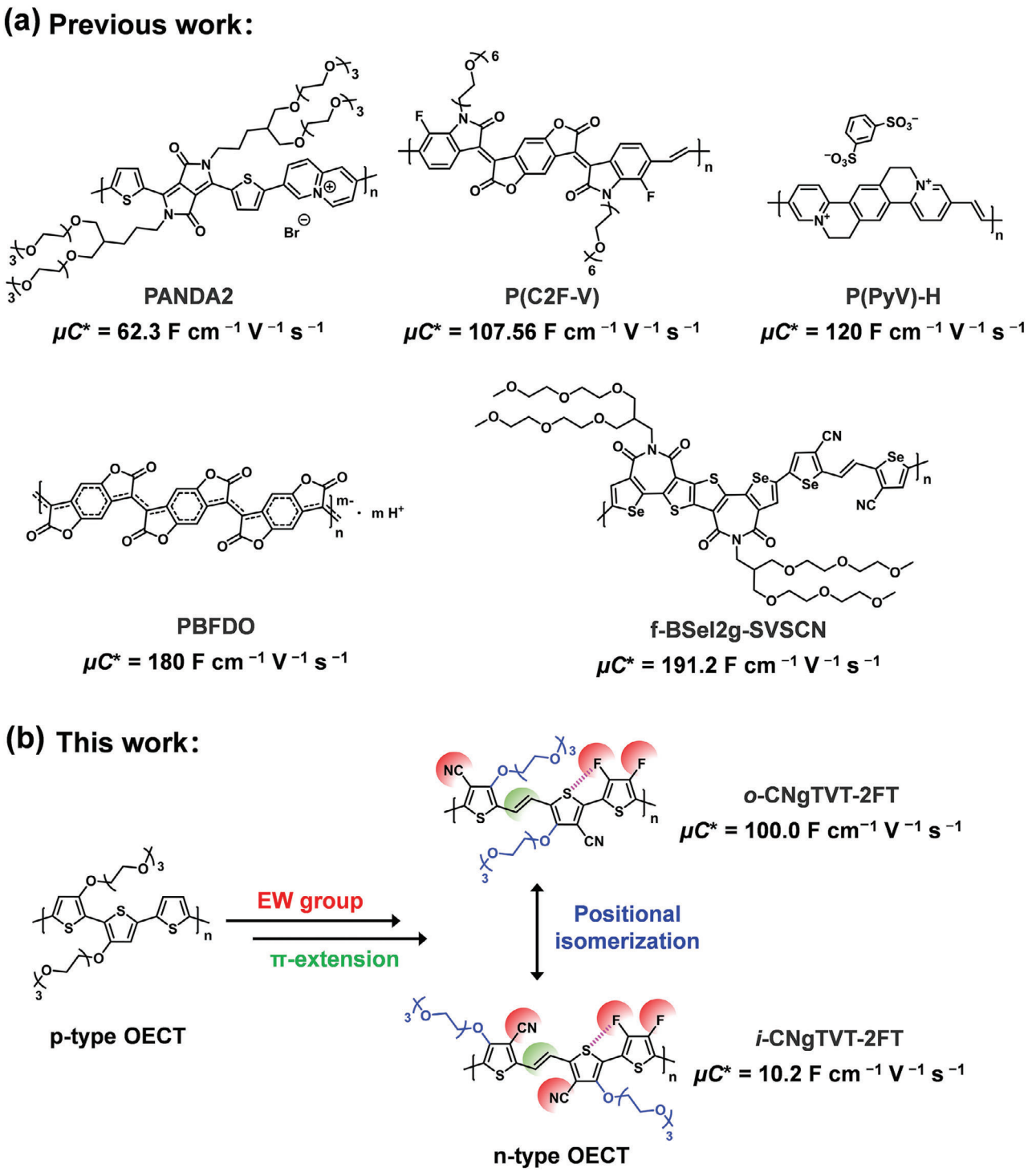

Figure 1. a) Typical chemical structures of high-performance n-type OECT polymers with the figure of merit (μC^*) over 50 F cm^{-1} V^{-1} s^{-1} reported in the literature.[41–43,45,46] b) Molecular design strategies of polymers *o*-CNgTVT-2FT and *i*-CNgTVT-2FT in this work.

Supporting Information).[27,41–46] Besides, most of these polymers have complex structures and long synthetic routes, facing challenges for low-cost applications.

Polythiophene and its derivatives possess simple chemical structures but always function as p-type OECT materials. To date, p-type polythiophene-based OECT materials have been well-developed and achieved exceptional performance with μC^* over several hundred F cm^{-1} V^{-1} s^{-1}.[18,20,47,48] However, the exploration of n-type polythiophene remains restricted due to the electron-rich nature of thiophene. To date, very

few polythiophene-based n-type OECT materials have been developed with a relatively low μC^* of 27.01 F cm^{-1} V^{-1} s^{-1}, and unsatisfactory stability with only 80% current retention after 2400 s switching operation.[49] Such performance is non-competitive compared to the state-of-the-art n-type polymeric semiconductors.[42,43] Although there are a few examples of n-type polythiophene in organic field-effect electrochemical transistors (OFETs), the performance remains poor with low electron mobility (μ_e).[50,51] By introducing strong electron-withdrawing (EW) groups to lower the LUMO energy levels of polymers to avoid carriers trapped by H_2O/O_2, the stability of n-type OFET materials can be effectively improved.[52–54] However, the design strategies for OFET materials cannot be directly applied to OECT materials, as the polymer films in OECTs are highly doped during operation. Therefore, the design strategies for high-performance n-type thiophene OECT polymers with both high μC^* and high stability still require further exploration.

Here, we report that a synergy of introducing electron-withdrawing (EW) groups, controlling polaron delocalization, and tuning molecular packing could convert p-type polythiophenes to high-performance n-type OECT materials. We designed and synthesized two novel regioisomeric polythiophene derivative isomers, *o*-CNgTVT-2FT and *i*-CNgTVT-2FT (**Figure** 1b), distinguished by the relative positions of the cyano groups and the ethylene glycol (EG) side chains. Both polymers displayed typical n-type OECT characteristics. Compared to *i*-CNgTVT-2FT, *o*-CNgTVT-2FT showed more delocalized and stabilized negative charges, efficient 3D charge transport channels, and smooth film morphology. As a result, *o*-CNgTVT-2FT achieved excellent μC^* of up to 100.0 F cm^{-1} V^{-1} s^{-1} and high electron mobility (μ_e) of 0.517 cm^2 V^{-1} s^{-1}, comparable to the recently reported state-of-the-art n-type OECT polymers based on fused aromatic rings. This polymer also exhibited remarkable OECT operational stability, with 93.6% current retention after 1000 switching cycles in the air, among the most stable n-type OECT materials with $\mu C^* > 50$ F cm^{-1} V^{-1} s^{-1}. Our results underscore that polythiophene and its derivatives could be considered promising n-type OECT materials with both high μC^* and high operational stability.

2. Results and Discussion

2.1. Polymer Design and Synthesis

Unlike conventional n-type OECT materials with complex fused aromatic rings (**Figure** 1a), we elaborately designed polythiophene polymers as n-type OECT materials using a synergistic strategy (**Figure** 1b). Vinylene spacer groups were incorporated into polythiophene to extend the π-conjugation length. First, the cyano and fluorine groups were chosen as the EW groups to lower the frontier molecular orbitals (FMOs) energy level and promote electron injection. Previous studies have revealed that controlling polarons distribution and delocalization on diketopyrrolopyrrole-based donor-acceptor (D-A) polymer backbone could enhance carrier mobility and stability.[27,39,55] However, related research based on n-type polythiophene systems has not been reported yet. Hence these groups were strategically grafted onto each thiophene unit to enhance negative polaron delocalization and stability. Fluorine functionalization could also induce intramolecular or intermolecular F···S interactions, improving the planarity of the backbone and promoting favorable molecular packing. Side chains play an important role in polymer film morphology and mixed conduction properties in OECTs. Fine-tuning the length and density of side chains has been shown to significantly improve the μC^* of n-type polymers.[35,56] Herein, we choose triethylene glycol chains as solubilizing groups of the polymers due to their abilities to facilitate sufficient ionic penetration while maintaining facile electronic charge transport properties.[18,48,55] It is well known that the performance of polythiophene is strongly dependent on its crystallization and packing behavior.[57,58] To tune molecular packing, the regioselective synthetic strategy by the positional isomerization of the cyano groups and ethylene glycol (EG) side chain was applied to design the polymers. Based on these strategies, we synthesized two polythiophene derivatives, *o*-CNgTVT-2FT and *i*-CNgTVT-2FT.

The chemical structures and synthetic routes for the monomers and corresponding polymers are shown in **Scheme** 1 and Figure S1 (Supporting Information). Compound **3** was obtained by the McMurray coupling reaction of compound **2**. After bromination, a base-catalyzed halogen dance (BCHD) reaction yielded compound **5**. Then, cyanation using CuCN as the cyano source yielded *o*-CNgTVT with a high yield of 82%. Notably, attempts to brominate the thiophene α-positions of *o*-CNgTVT using conventional reagents like NBS or bromine failed, possibly due to the high electron deficiency. The dibrominated monomer *o*-CNgTVT-2Br was synthesized by the lithiation of *o*-CNgTVT, followed by a reaction with 1,2-dibromo-1,1,2,2-tetrachloroethane, yielding 86%. The synthetic route of *i*-CNgTVT-2Br is similar to *o*-CNgTVT-2Br. Compound **9** was prepared via McMurray coupling reaction, followed by cyanation and desilylation, obtaining *i*-CNgTVT with an 80% yield over two steps. Bromination of *i*-CNgTVT using NBS afforded *i*-CNgTVT-2Br a good yield of 87%. Copolymers *o*-CNgTVT-2FT and *i*-CNgTVT-2FT were synthesized via typical Stille coupling polymerization between the brominated monomers *o*-CNgTVT-2Br/*i*-CNgTVT-2Br, and the distannylated difluorothiophene comonomer (2FT-2Sn). The polymers were purified by successive Soxhlet extraction, and the chloroform fractions were collected. The incorporation of triethylene glycol side chains endows the two polymers with excellent solubility. Both polymers exhibited good thermal stabilities (T_d) with 5% weight loss temperatures over 300 °C, as estimated by thermogravimetric analysis (TGA) under an N_2 atmosphere (Figure S2, Supporting Information). Differential scanning calorimetry (DSC) showed no distinctive thermal transition in the temperature range of 30–260 °C (Figure S3, Supporting Information).

2.2. Electrochemical Properties and OECT Device Performance

The optical properties of *o*-CNgTVT-2FT and *i*-CNgTVT-2FT were evaluated by UV−vis absorption spectroscopy (**Figure** 2a). Both polymers exhibited absorption between 300–900 nm in dilute solutions and red-shifted absorption spectra in the solid state, suggesting stronger aggregation and interchain stacking in the solid state. The optical band gaps of *o*-CNgTVT-2FT and *i*-CNgTVT-2FT calculated from the absorption onset of the films are 1.65 and 1.59 eV, respectively (**Table** 1). To

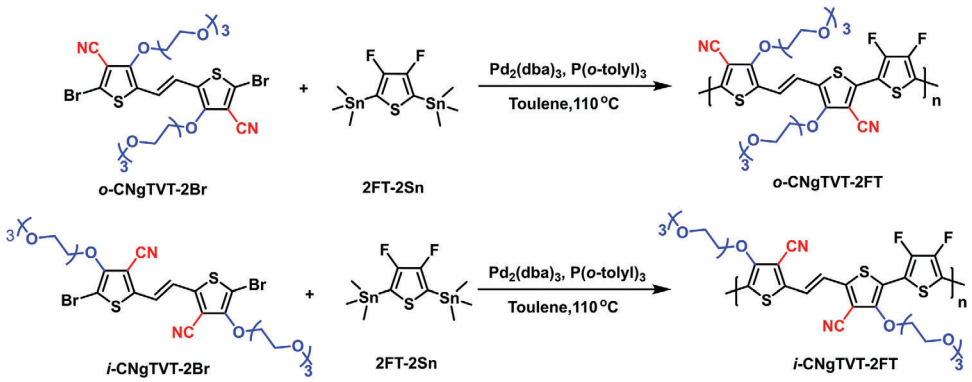

Scheme 1. The synthetic route to polymers *o*-CNgTVT-2FT and *i*-CNgTVT-2FT.

investigate the electrochemical properties of the two polymers, cyclic voltammetry (CV) was performed in a 0.1 M acetonitrile solution of tetrabutylammonium hexafluorophosphate (*n*-Bu_4NPF_6) (**Figure** 2b). The lowest unoccupied molecular orbital (LUMO)/highest occupied molecular orbital (HOMO) levels for *o*-CNgTVT-2FT and *i*-CNgTVT-2FT were calculated to be −3.74/−5.49 and −3.80/−5.50 eV, respectively (**Table** 1), aligning with density-functional theory (DFT) calculation results (Figure S4, Supporting Information). DFT calculations also revealed that two polymers have highly planar geometries with small dihedral angles (< 3°) between adjacent thiophene rings. The F···S distances in *o*-CNgTVT-2FT (2.86 Å) and *i*-CNgTVT-2FT (2.93 Å) were shorter than the sum of F···S van der Waals radii (3.27 Å), indicating the formation of intramolecular noncovalent F···S interactions. Besides, a shorter O···S distance of 2.86 Å was observed in *i*-CNgTVT-2FT which confirmed the presence of intramolecular locks provided by the O···S interactions. These intramolecular interactions are beneficial to planarize the π-conjugated backbone, thus facilitating charge transport.[59,60]

During continuous CV sweep measurements over 10 doping/de-doping cycles in 0.1 M NaCl aqueous solution (**Figure** 2c,d), *o*-CNgTVT-2FT presented better electrochemical stability, making it more favorable for operational stability in OECT devices. The reduction onsets were −0.55 V for

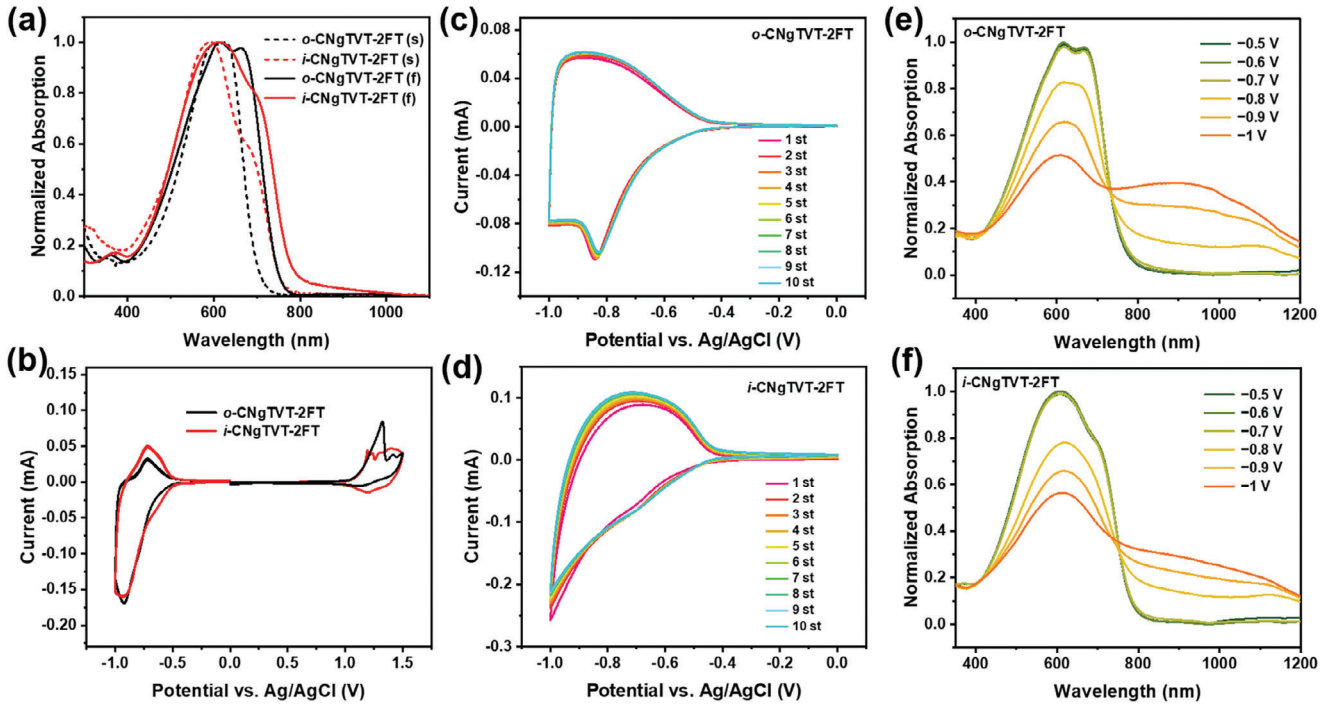

Figure 2. a) Normalized UV–vis–NIR absorption spectra of polymers in chloroform solution (10^{-5} M) and films. b) Film cyclic voltammograms (CV) of polymers in 0.1 M tetrabutylammonium hexafluorophosphate (*n*-Bu_4NPF_6) acetonitrile solution with Fc/Fc^+ as an external standard. Film CV of c) *o*-CNgTVT-2FT and d) *i*-CNgTVT-2FT in 0.1 M NaCl aqueous solution with a negative potential between 0 and −1.0 V for 10 cycles. Electrochemical absorption spectra of e) *o*-CNgTVT-2FT and f) *i*-CNgTVT-2FT films in 0.1 M NaCl aqueous solution with a negative potential between −0.5 and −1.0 V versus Ag/AgCl.

Table 1. Physicochemical properties of *o*-CNgTVT-2FT and *i*-CNgTVT-2FT.

Polymer	λ_{max}^{sol} [nm]	λ_{max}^{film} [nm]	E_g^{opt} [eV]	E_g^{CV} [eV]	E_{HOMO}^{CV} [eV]	E_{LUMO}^{CV} [eV]
o-CNgTVT-2FT	601	614	1.65	1.75	−5.49	−3.74
i-CNgTVT-2FT	590	612	1.59	1.70	−5.50	−3.80

i-CNgTVT-2FT and −0.57 V for *o*-CNgTVT-2FT (Figure S5, Supporting Information), showing a positive shift than in organic electrolytes, which is due to the changes in counterion size, charge density, and solute-solvent interactions.[15,55] The ionic doping characteristics of two polymers were further investigated by spectroelectrochemistry (**Figure 2e,f**; Figure S6, Supporting Information). Both polymers exhibited electrochromic properties and similar changes in absorption spectra. The absorption peaks remained stable up to −0.7 V versus Ag/AgCl, then gradually decreased while polaronic absorption increased at the long wavelength of 800–1200 nm, demonstrating effective doping.[61] For a more quantitative comparison, the absorbance relative changes of the π–π^* peaks at 608–616 nm and polaron peaks at 850–904 nm of each polymer film upon electrochemical doping at various voltages are shown in Figure S7 (Supporting Information). Both polymers showed similar bleaching, indicating their comparable doping efficiencies. These results suggest that the regiochemistry controlled by exchanging the position of the cyano groups and the polar side chains in the same polymer backbone has minimal impact on their electrochemical doping ability.

To investigate the electrical performance of the two polymers, OECT devices with a channel width/length (W/L) = 100/10 µm were fabricated using a photolithography and parylene patterning method. The semiconductor layers were obtained by spin-coating, and the devices were tested in 0.1 M NaCl solution using Ag/AgCl as the gate electrode (see more details in the Supporting Information, and the corresponding cross-sectional schematic of the OECT device is shown in Figure S8, Supporting Information).

Different from most polythiophenes and their derivatives that exhibit p-type characteristics, both *o*-CNgTVT-2FT and *i*-CNgTVT-2FT displayed typical n-type accumulation-mode properties (**Figure 3** and **Table 2**). Consistent with the CV results in the aqueous solution, two polymers showed similar V_{Th}, while *o*-CNgTVT-2FT exhibited a much higher μC^* of 100.0 F cm^{-1} V^{-1} s^{-1} and on/off current ratio of ≈10^7 compared to *i*-CNgTVT-2FT (only 10.2 F cm^{-1} V^{-1} s^{-1} and ≈10^5) (**Figure 3a,b**). For comparison, the geometry-normalized transconductance ($g_{m,norm} = g_m/(Wd/L)$) values were used, where *o*-CNgTVT-2FT reached a $g_{m,norm}$ of 17.4 S cm^{-1}, while *i*-CNgTVT-2FT yielded only 2.2 S cm^{-1}. Electrochemical impedance spectrum (EIS) measurement was employed to calculate the C^* values (Figure S9, Supporting Information). The C^* gradually increased with the increase of applied voltage, with maximum values of 193.3 F cm^{-3} for *o*-CNgTVT-2FT and 214.2 F cm^{-3} for *i*-CNgTVT-2FT.

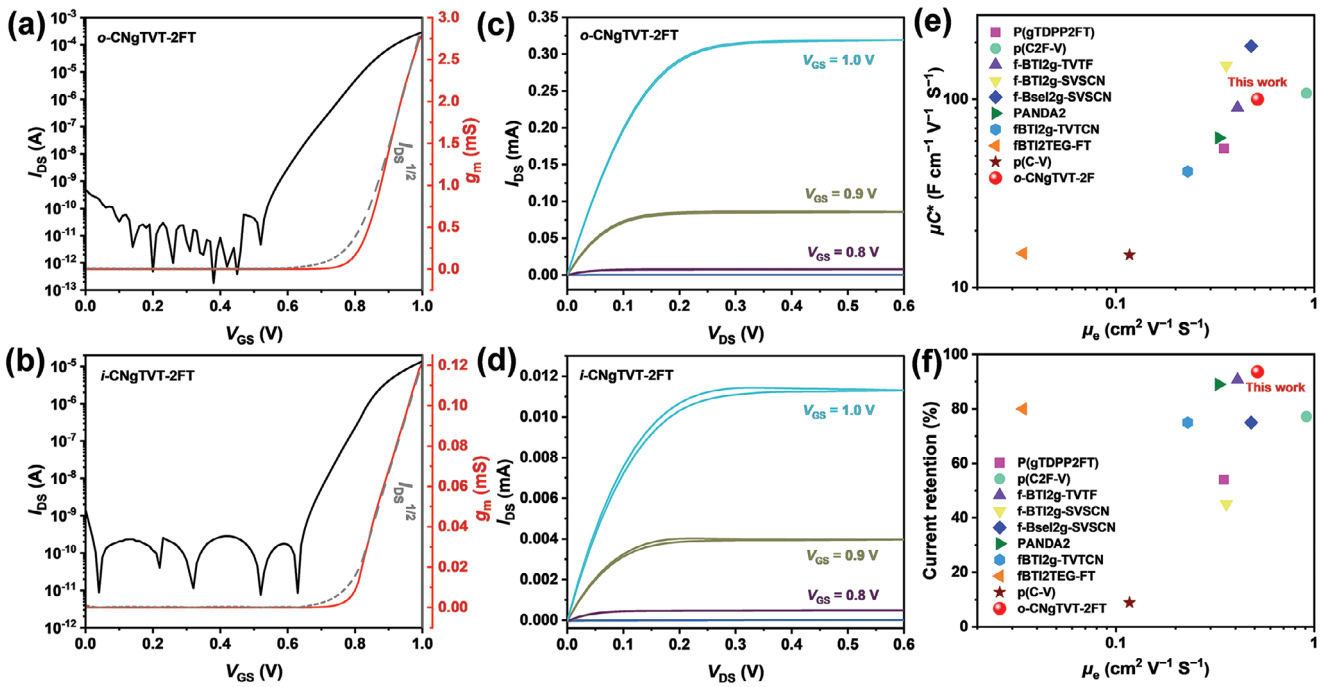

Figure 3. a,b) Transfer, transconductance characteristics and c,d) output characteristics of *o*-CNgTVT-2FT and *i*-CNgTVT-2FT. The dash lines are the curve of linear $I_{DS}^{1/2}$ versus V_{GS}. W/L = 100/10 µm, V_{DS} = 0.6 V. Comparison of the e) μC^* and μ_e, and f) current retention values and μ_e of *o*-CNgTVT-2FT with other reported n-type OECT materials.[27,41–44,64,65]

Table 2. Summary of Performance Parameters of OECT based on *o*-CNgTVT-2FT and *i*-CNgTVT-2FT.

Polymer	$g_{m,\,norm}$ [S cm^{-1}]	V_{Th} [V]	μC^* [F cm^{-1} V^{-1} s^{-1}]	μ_e [cm^2 V^{-1} s^{-1}]	C^* [F cm^{-3}]	τ_{on} [ms]	τ_{off} [ms]
o-CNgTVT-2FT	17.4	0.79	100.0 (88.2 ± 7.2)	0.517 (0.456 ± 0.039)	193.3 ± 5.2	2.86	0.33
i-CNgTVT-2FT	2.2	0.78	10.2 (8.33 ± 1.1)	0.048 (0.039 ± 0.010)	214.2 ± 49.6	3.92	0.60

These results correlated well with the spectroelectrochemistry measurements that both polymers show similar bleaching levels at different voltage bias. It is worth noting that we employed the Randles circuit model, which is most commonly used in literature, to extract the capacitance from the EIS data.[20,42,62] And the offset of the fit may originate from ion injection barriers or ion accumulation at the polymer film/electrolyte interface.[63] Based on the μC^* and C^* values, we calculated μ_e and surprisingly found that the *o*-CNgTVT-2FT showed ≈12 times higher μ_e (0.517 cm^2 V^{-1} s^{-1}) than *i*-CNgTVT-2FT (0.048 cm^2 V^{-1} s^{-1}). Such high μ_e and μC^* of *o*-CNgTVT-2FT are comparable to recently reported state-of-the-art fused-ring n-type OECT polymers (**Figure** 3e; Table S1, Supporting Information).[29,41,42] Note that to conduct a fair performance comparison, we fabricated OECT devices based on the two polymers under identical processing conditions. It could be found that the film thicknesses were 159 nm for *o*-CNgTVT-2FT and 55 nm for *i*-CNgTVT-2FT, respectively. The discrepancy in film thickness may originate from differences in their molecular weights. Of course, similar film thicknesses could be achieved by tuning the concentrations of polymer solution.

The operational stability and response time are of great importance for practical applications. The OECT device based on *o*-CNgTVT-2FT showed a significantly higher current retention of 93.6% than *i*-CNTVT-2FT of 47.9% after 1000 switching cycles (2000 s) measurement in air (**Figure** 4a,b). The outstanding stability of *o*-CNgTVT-2FT surpasses all other reported high-performance n-type OECT polymers with $\mu C^* > 50$ F cm^{-1} V^{-1} s^{-1} (**Figure** 3f; Table S1, Supporting Information). The transient characteristics of both polymers were evaluated by applying a 1.0 V pulse to the gate (40 ms) and a 0.6 V DC voltage to the drain electrode. The response time was extracted by the exponential fit to the I_{DS} curve, which afforded on/off time constants (τ_{on}/τ_{off}) of 2.86/0.33 ms for *o*-CNgTVT-2FT, and 3.92/0.60 ms for *i*-CNgTVT-2FT, respectively (**Figure** 4e,f). In brief, our design strategy successfully converted the p-type polythiophene material into high-performance n-type OECT material, and *o*-CNgTVT-2FT, shows high μC^* and exceptional operational stability, and fast response speed.

2.3. Film Microstructure Characterization and Doped State Analysis

To understand the structure-property relationship between the two polymers, we conducted a series of characterizations. First,

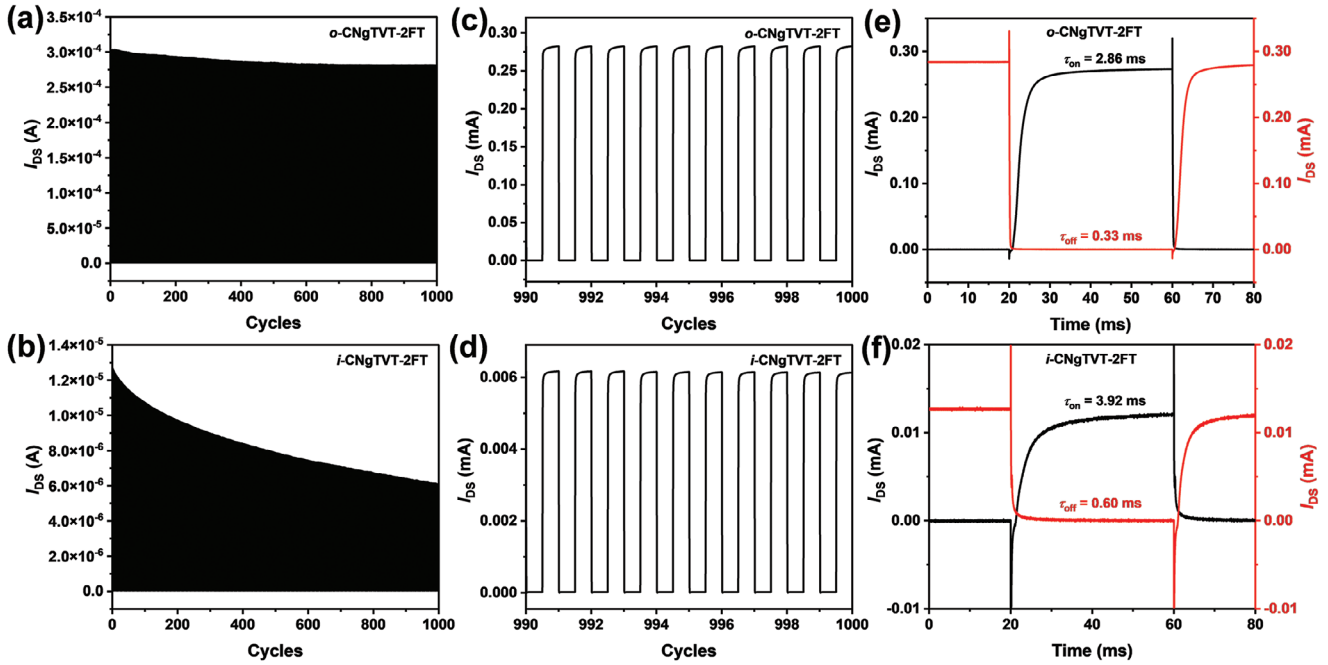

Figure 4. a,b) Long-term operational stability under a gate voltage pulse for 1000 cycles and c,d) 10 cycles enlargement from 990 to 1000 cycles of *o*-CNgTVT-2FT and *i*-CNgTVT-2FT (V_{GS} = 0.3–1.0 V, V_{DS} = 0.6 V, pulse length = 1 s). e,f) Transient on/off curves of *o*-CNgTVT-2FT and *i*-CNgTVT-2FT (V_{GS} = 0–1.0 V. V_{DS} = 0.6 V).

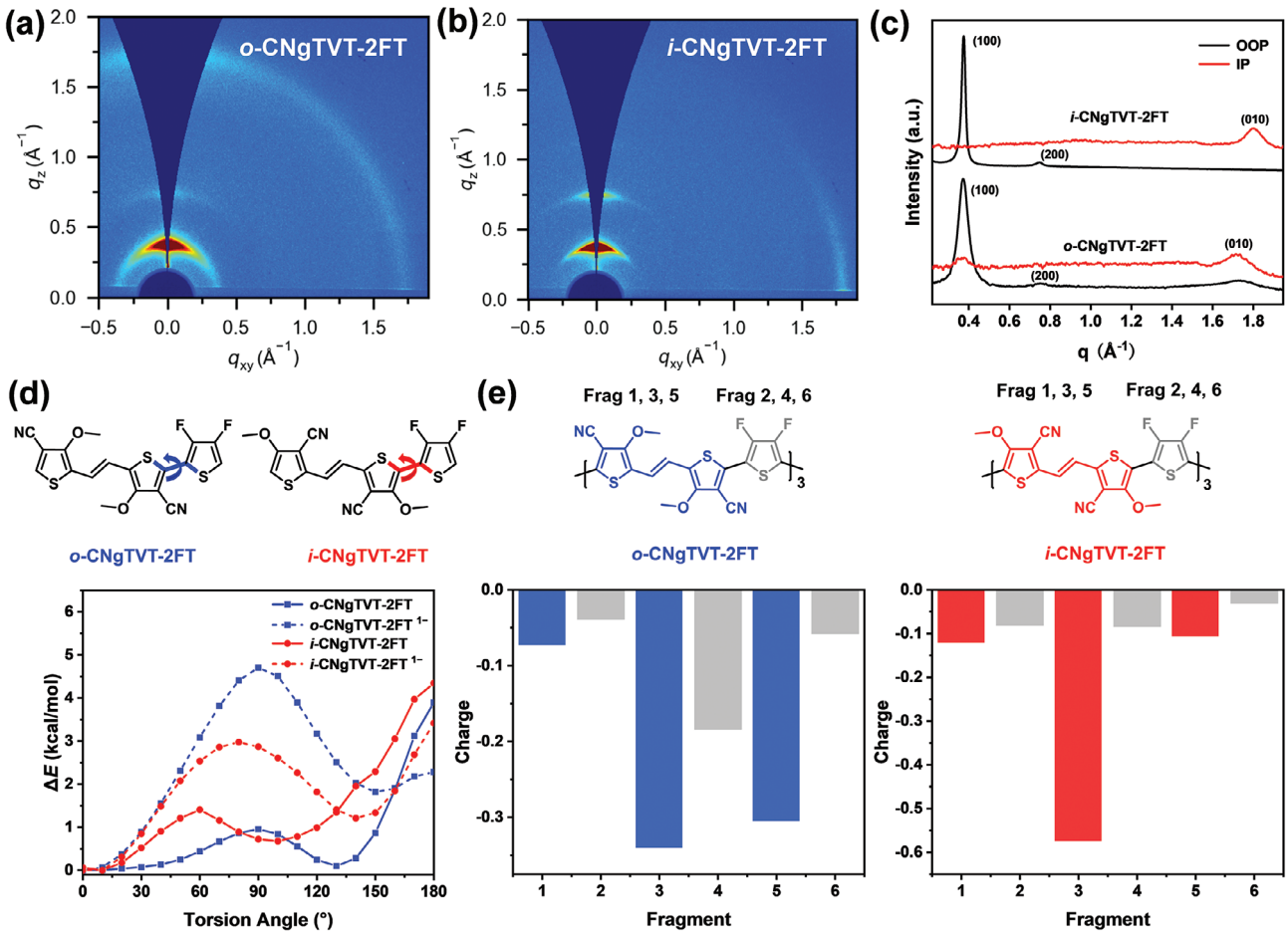

Figure 5. a,b) 2D GIWAXS patterns and c) corresponding 1D in-plane and out-of-plane plots of *o*-CNgTVT-2FT and *i*-CNgTVT-2FT films. d) Comparison of the relaxed potential energy surface (PES) scans of the dihedral angles for the repeating units of *o*-CNgTVT-2FT and *i*-CNgTVT-2FT in neutral and reduced states. e) Details about the fragmentation of the trimers into shorter segments and DFT calculations of the charge distributions over the negatively charged trimer fragments of *o*-CNgTVT-2FT and *i*-CNgTVT-2FT in vacuum. The charges of the reduced state minus the neutral state obtained every fragment charge.

atomic force microscopy (AFM) and grazing-incidence wide-angle X-ray scattering (GIWAXS) were employed to elucidate the molecular packing and microstructure of both polymers. Several studies have demonstrated that modifying the ethylene glycol (EG) side chains of polymers with the same backbone (e.g., composition,[66] length,[67] symmetry,[34] and position relative to the backbone)[35] could also significantly affect film morphology, thereby influencing their charge transport properties in OECTs. For *o*-CNgTVT-2FT and *i*-CNgTVT-2FT, AFM results showed that relative to the initial neat film, both polymer films exhibited a minimal change in morphology after exposure to the electrolyte. Moreover, following electrochemical reduction and the removal of voltage, the morphology of both polymers remained unchanged, retaining similar continuous microfibrillar structures, thereby demonstrating their excellent morphological stability (Figures S10 and S11, Supporting Information). Moreover, *o*-CNgTVT-2FT displayed a smoother surface with smaller roughness than *i*-CNgTVT-2FT, which may be related to different molecular packing behaviors and the difference in molecular weights. 2D GIWAXS diffraction patterns confirmed that *i*-CNgTVT-2FT showed a typical edge-on packing, while *o*-CNgTVT-2FT showed a mixed edge-on and face-on packing (**Figure** 5a–c and Table S2, Supporting Information). The face-on oriented crystallites of *o*-CNgTVT-2FT signified a parallel arrangement of polymer hydrophobic aromatic backbone relative to the substrate, potentially enhancing the hydrophobicity, which is consistent with its larger contact angle (Figure S12, Supporting Information). Compared with *o*-CNgTVT-2FT, *i*-CNgTVT-2FT exhibited shorter π–π stacking distance and longer π–π stacking coherence length in the IP direction, and shorter lamellar distance in the OOP direction, indicating a denser intermolecular packing and enhanced film crystallinity of *i*-CNgTVT-2FT. It could be attributed to the better conformational uniformity of *i*-CNgTVT-2FT, as will be discussed in the following DFT analysis. Note that the mixed face-on and edge-on molecular stacking of *o*-CNgTVT-2FT facilitates the formation of efficient 3D charge transport channels, promoting bulk molecular doping in OECTs[32,36,67] and leading to higher electron mobility. However, its larger contact angle may be detrimental to ion penetration. Additionally, for *i*-CNgTVT-2FT, its high crystallinity may

hinder ion insertion into the polymer film, despite having a smaller water contact angle. These factors collectively result in *o*-CNgTVT-2FT and *i*-CNgTVT-2FT exhibiting similar initial reduction voltages and C^*. These results indicate that the regiochemistry strategy for adjusting molecular packing is an effective and feasible approach for designing thiophene-based n-type OECT materials.

The characteristics of the two polymers in the doped state were calculated and analyzed for a better understanding. We performed relaxed potential energy surface (PES) scans of the dihedral angle between difluorothiophene and its adjacent thiophene unit of the two polymers in neutral and charged states (**Figure** 5d). In the neutral state, *o*-CNgTVT-2FT exhibited two energy minima at 0° and 130° with an energy difference of 0.1 kcal mol^{-1}, while *i*-CNgTVT-2FT showed a dominant conformation at 10° with a much higher energy barrier of 1.2 kcal mol^{-1}. Notably, both polymers showed the most stable conformation at 0° when negatively charged, but *o*-CNgTVT-2FT showed an ≈1.6 times higher torsional barrier compared to *i*-CNgTVT-2FT (4.70 vs 2.97 kcal mol^{-1}). This result indicated that *o*-CNgTVT-2FT has a more planar and rigid backbone structure in the reduced state. Additionally, both polymers showed similar Gibbs free energy changes (ΔG) from the neutral to the reduced state in a vacuum or H_2O environment, and their spin densities distributed along the entire polymer backbone, demonstrating that introducing electron-withdrawing substituents to each thiophene unit can effectively promote negative polaron delocalization (Figures S13 and S14, Supporting Information). For further support, charge distributions of the two polymers relative to their neutral state were calculated. As shown in **Figure** 5e and Figure S15 (Supporting Information), *o*-CNgTVT, and *i*-CNgTVT moieties carried more charges than the difluorothiophene units due to their more extended conjugated backbones. Unlike *i*-CNgTVT-2FT, where negative polarons are predominantly localized on a single *i*-CNgTVT fragment at the trimer center, *o*-CNgTVT-2FT exhibited charges distributed across the two *o*-CNgTVT units and spreading to the central 2FT group and other parts of the chain. This suggests a more delocalized charge distribution across the polymer chain of *o*-CNgTVT-2FT compared to *i*-CNgTVT-2FT both in vacuum and aqueous environments, indicating that polaron delocalization could be efficiently regulated by controlling regiochemistry with the same polymer backbone. Previous studies have reported that charge delocalization and reduced torsional disorder conduce to high charge carrier mobilities and polaron stabilization.[18,68,69] The calculation results demonstrated that *o*-CNgTVT-2FT showed better backbone planarity, a higher torsion energy barrier, and more delocalized polarons in the doped state, which well explained its higher μ_e and better operational stability. Besides, GIWAXS analysis revealed that *o*-CNgTVT-2FT featured mixed face-on and edge-on molecular packing with lower crystallinity, which may help retain good film microstructure after doping,[62] thus enhancing stability.

3. Conclusion

In summary, without using fused aromatic rings, we successfully converted conventional p-type polythiophenes into high-performance n-type OECT materials by combining electron-withdrawing groups, optimizing polaron delocalization, and tuning molecular packing. By controlling regiochemistry, we effectively regulated the molecular packing, film morphology, and also the doped state properties of the polymers. As a result, *o*-CNgTVT-2FT-based OECTs realized superior n-type OECT performance with a high μC^* of 100.0 F cm^{-1} V^{-1} s^{-1} and excellent operational stability of 93.6% current retention after 1000 electrochemical switching cycles. To our knowledge, the polymer exhibits the best stability among high-performance n-type OECT materials with $\mu C^* > 50$ F cm^{-1} V^{-1} s^{-1}. Our work reveals the great potential of using simple polythiophene derivatives for high-performance and stable n-type OECT materials and enriches our understanding of the structure-property relationship in n-type OECTs.

Supporting Information

Supporting Information is available from the Wiley Online Library or from the author.

Acknowledgements

C.Z. and Y.Z. contributed equally to this work. The authors are grateful to the National Natural Science Foundation of China (21975176, T2425010, and 5240031308). The authors thank the Seed Foundation of Tianjin University (No. 2024XJD-0058) and the Haihe Laboratory of Sustainable Chemical Transformations (24HHWCSS00009) for financial support. The GIWAXS measurement is performed on the BL14B1 beamline of the Shanghai Synchrotron Radiation Facility.

Conflict of Interest

The authors declare no conflict of interest.

Data Availability Statement

The data that support the findings of this study are available from the corresponding author upon reasonable request.

Keywords

electron-withdrawing groups, n-type conjugated polymers, organic electrochemical transistors, polythiophenes, regiochemistry control

Received: October 17, 2024
Revised: January 12, 2025
Published online:

[1] M. Berggren, A. Richter-Dahlfors, *Adv. Mater.* **2007**, *19*, 3201.
[2] M. Ghittorelli, L. Lingstedt, P. Romele, N. I. Crăciun, Z. M. Kovács-Vajna, P. W. M. Blom, F. Torricelli, *Nat. Commun.* **2018**, *9*, 1441.
[3] D. Khodagholy, J. Rivnay, M. Sessolo, M. Gurfinkel, P. Leleux, L. H. Jimison, E. Stavrinidou, T. Herve, S. Sanaur, R. M. Owens, G. G. Malliaras, *Nat. Commun.* **2013**, *4*, 2133.
[4] J. Rivnay, S. Inal, A. Salleo, R. M. Owens, M. Berggren, G. G. Malliaras, *Nat. Rev. Mater.* **2018**, *3*, 17086.
[5] P. Lin, F. Yan, *Adv. Mater.* **2012**, *24*, 34.

[6] D. Ohayon, G. Nikiforidis, A. Savva, A. Giugni, S. Wustoni, T. Palanisamy, X. Chen, I. P. Maria, E. Di Fabrizio, P. M. F. J. Costa, I. McCulloch, S. Inal, *Nat. Mater.* **2020**, *19*, 456.
[7] R. A. Picca, K. Manoli, E. Macchia, L. Sarcina, C. Di Franco, N. Cioffi, D. Blasi, R. Österbacka, F. Torricelli, G. Scamarcio, L. Torsi, *Adv. Funct. Mater.* **2020**, *30*, 1904513.
[8] S. Inal, J. Rivnay, A.-O. Suiu, G. G. Malliaras, I. McCulloch, *Acc. Chem. Res.* **2018**, *51*, 1368.
[9] R. B. Rashid, X. Ji, J. Rivnay, *Biosens. Bioelectron.* **2021**, *190*, 113461.
[10] T. Arbring Sjöström, M. Berggren, E. O. Gabrielsson, P. Janson, D. J. Poxson, M. Seitanidou, D. T. Simon, *Adv. Mater.Technol.* **2018**, *3*, 1700360.
[11] P. C. Harikesh, C.-Y. Yang, D. Tu, J. Y. Gerasimov, A. M. Dar, A. Armada-Moreira, M. Massetti, R. Kroon, D. Bliman, R. Olsson, E. Stavrinidou, M. Berggren, S. Fabiano, *Nat. Commun.* **2022**, *13*, 901.
[12] Y. van de Burgt, E. Lubberman, E. J. Fuller, S. T. Keene, G. C. Faria, S. Agarwal, M. J. Marinella, A. Alec Talin, A. Salleo, *Nat. Mater.* **2017**, *16*, 414.
[13] A. Williamson, M. Ferro, P. Leleux, E. Ismailova, A. Kaszas, T. Doublet, P. Quilichini, J. Rivnay, B. Rózsa, G. Katona, C. Bernard, G. G. Malliaras, *Adv. Mater.* **2015**, *27*, 4405.
[14] B. D. Paulsen, K. Tybrandt, E. Stavrinidou, J. Rivnay, *Nat. Mater.* **2020**, *19*, 13.
[15] J. Chen, S. Cong, L. Wang, Y. Wang, L. Lan, C. Chen, Y. Zhou, Z. Li, I. McCulloch, W. Yue, *Mater. Horiz* **2023**, *10*, 607.
[16] J. Rivnay, S. Inal, B. A. Collins, M. Sessolo, E. Stavrinidou, X. Strakosas, C. Tassone, D. M. Delongchamp, G. G. Malliaras, *Nat. Commun.* **2016**, *7*, 11287.
[17] Y. Wang, L. Feng, S. Wang, *Adv. Funct. Mater.* **2019**, *29*, 1806818.
[18] R. K. Hallani, B. D. Paulsen, A. J. Petty, R. Sheelamanthula, M. Moser, K. J. Thorley, W. Sohn, R. B. Rashid, A. Savva, S. Moro, J. P. Parker, O. Drury, M. Alsufyani, M. Neophytou, J. Kosco, S. Inal, G. Costantini, J. Rivnay, I. McCulloch, *J. Am. Chem. Soc.* **2021**, *143*, 11007.
[19] I.-Y. Jo, D. Jeong, Y. Moon, D. Lee, S. Lee, J.-G. Choi, D. Nam, J. H. Kim, J. Cho, S. Cho, D.-Y. Kim, H. Ahn, B. J. Kim, M.-H. Yoon, *Adv. Mater.* **2024**, *36*, 2307402.
[20] M. Moser, T. C. Hidalgo, J. Surgailis, J. Gladisch, S. Ghosh, R. Sheelamanthula, Q. Thiburce, A. Giovannitti, A. Salleo, N. Gasparini, A. Wadsworth, I. Zozoulenko, M. Berggren, E. Stavrinidou, S. Inal, I. McCulloch, *Adv. Mater.* **2020**, *32*, 2002748.
[21] A. Giovannitti, C. B. Nielsen, D.-T. Sbircea, S. Inal, M. Donahue, M. R. Niazi, D. A. Hanifi, A. Amassian, G. G. Malliaras, J. Rivnay, I. McCulloch, *Nat. Commun.* **2016**, *7*, 13066.
[22] M. Kawan, T. C. Hidalgo, W. Du, A.-M. Pappa, R. M. Owens, I. McCulloch, S. Inal, *Mater. Horiz.* **2020**, *7*, 2348.
[23] P. Romele, P. Gkoupidenis, D. A. Koutsouras, K. Lieberth, Z. M. Kovács-Vajna, P. W. M. Blom, F. Torricelli, *Nat. Commun.* **2020**, *11*, 3743.
[24] H. Sun, M. Vagin, S. Wang, X. Crispin, R. Forchheimer, M. Berggren, S. Fabiano, *Adv. Mater.* **2018**, *30*, 1704916.
[25] C.-Y. Yang, D. Tu, T.-P. Ruoko, J. Y. Gerasimov, H.-Y. Wu, P. C. Harikesh, M. Massetti, M.-A. Stoeckel, R. Kroon, C. Müller, M. Berggren, S. Fabiano, *Adv. Electron. Mater.* **2022**, *8*, 2100907.
[26] X. Ji, X. Lin, J. Rivnay, *Nat. Commun.* **2023**, *14*, 1665.
[27] P. Li, J. Shi, Y. Lei, Z. Huang, T. Lei, *Nat. Commun.* **2022**, *13*, 5970.
[28] Y. Wang, G. Zhu, E. Zeglio, T. C. H. Castillo, S. Haseena, M. K. Ravva, S. Cong, J. Chen, L. Lan, Z. Li, A. Herland, I. McCulloch, S. Inal, W. Yue, *Chem. Mater.* **2023**, *35*, 405.
[29] Y. Wang, E. Zeglio, L. Wang, S. Cong, G. Zhu, H. Liao, J. Duan, Y. Zhou, Z. Li, D. Mawad, A. Herland, W. Yue, I. McCulloch, *Adv. Funct. Mater.* **2022**, *32*, 2111439.
[30] K. Feng, W. Shan, S. Ma, Z. Wu, J. Chen, H. Guo, B. Liu, J. Wang, B. Li, H. Y. Woo, S. Fabiano, W. Huang, X. Guo, *Angew. Chem., Int. Ed.* **2021**, *60*, 24198.
[31] H.-Y. Wu, C.-Y. Yang, Q. Li, N. B. Kolhe, X. Strakosas, M.-A. Stoeckel, Z. Wu, W. Jin, M. Savvakis, R. Kroon, D. Tu, H. Y. Woo, M. Berggren, S. A. Jenekhe, S. Fabiano, *Adv. Mater.* **2022**, *34*, 2106235.
[32] X. Chen, A. Marks, B. D. Paulsen, R. Wu, R. B. Rashid, H. Chen, M. Alsufyani, J. Rivnay, I. McCulloch, *Angew. Chem., Int. Ed.* **2021**, *60*, 9368.
[33] A. Erhardt, A. Hochgesang, C. R. McNeill, M. Thelakkat, *Adv. Electron. Mater.* **2023**, *9*, 2300026.
[34] D. Jeong, I.-Y. Jo, S. Lee, J. H. Kim, Y. Kim, D. Kim, J. R. Reynolds, M.-H. Yoon, B. J. Kim, *Adv. Funct. Mater.* **2022**, *32*, 2111950.
[35] I. P. Maria, B. D. Paulsen, A. Savva, D. Ohayon, R. Wu, R. Hallani, A. Basu, W. Du, T. D. Anthopoulos, S. Inal, J. Rivnay, I. McCulloch, A. Giovannitti, *Adv. Funct. Mater.* **2021**, *31*, 2008718.
[36] A. Marks, X. Chen, R. Wu, R. B. Rashid, W. Jin, B. D. Paulsen, M. Moser, X. Ji, S. Griggs, D. Meli, X. Wu, H. Bristow, J. Strzalka, N. Gasparini, G. Costantini, S. Fabiano, J. Rivnay, I. McCulloch, *J. Am. Chem. Soc.* **2022**, *144*, 4642.
[37] D. Ohayon, A. Savva, W. Du, B. D. Paulsen, I. Uguz, R. S. Ashraf, J. Rivnay, I. McCulloch, S. Inal, *ACS Appl. Mater. Interfaces* **2021**, *13*, 4253.
[38] Z. S. Parr, R. Halaksa, P. A. Finn, R. B. Rashid, A. Kovalenko, M. Weiter, J. Rivnay, J. Krajčovič, C. B. Nielsen, *ChemPlusChem* **2019**, *84*, 1384.
[39] J. Shi, P. Li, X.-Y. Deng, J. Xu, Z. Huang, Y. Lei, Y. Wang, J.-Y. Wang, X. Gu, T. Lei, *Chem. Mater.* **2022**, *34*, 864.
[40] Y. Zhang, G. Ye, T. P. A. van der Pol, J. Dong, E. R. W. van Doremaele, I. Krauhausen, Y. Liu, P. Gkoupidenis, G. Portale, J. Song, R. C. Chiechi, Y. van de Burgt, *Adv. Funct. Mater.* **2022**, *32*, 2201593.
[41] Z. Huang, P. Li, Y. Lei, X.-Y. Deng, Y.-N. Chen, S. Tian, X. Pan, X. Lei, C. Song, Y. Zheng, J.-Y. Wang, Z. Zhang, T. Lei, *Angew. Chem., Int. Ed.* **2024**, *63*, 202313260.
[42] W. Wu, K. Feng, Y. Wang, J. Wang, E. Huang, Y. Li, S. Y. Jeong, H. Y. Woo, K. Yang, X. Guo, *Adv. Mater.* **2024**, *36*, 2310503.
[43] Y. Wang, A. Koklu, Y. Zhong, T. Chang, K. Guo, C. Zhao, T. C. H. Castillo, Z. Bu, C. Xiao, W. Yue, W. Ma, S. Inal, *Adv. Funct. Mater.* **2024**, *34*, 2304103.
[44] W. Yang, K. Feng, S. Ma, B. Liu, Y. Wang, R. Ding, S. Y. Jeong, H. Y. Woo, P. K. L. Chan, X. Guo, *Adv. Mater.* **2024**, *36*, 2305416.
[45] H. Tang, Y. Liang, C. Liu, Z. Hu, Y. Deng, H. Guo, Z. Yu, A. Song, H. Zhao, D. Zhao, Y. Zhang, X. Guo, J. Pei, Y. Ma, Y. Cao, F. Huang, *Nature* **2022**, *611*, 271.
[46] P. Li, W. Sun, J. Li, J.-P. Chen, X. Wang, Z. Mei, G. Jin, Y. Lei, R. Xin, M. Yang, J. Xu, X. Pan, C. Song, X.-Y. Deng, X. Lei, K. Liu, X. Wang, Y. Zheng, J. Zhu, S. Lv, Z. Zhang, X. Dai, T. Lei, *Science* **2024**, *384*, 557.
[47] M. Moser, Y. Wang, T. C. Hidalgo, H. Liao, Y. Yu, J. Chen, J. Duan, F. Moruzzi, S. Griggs, A. Marks, N. Gasparini, A. Wadsworth, S. Inal, I. McCulloch, W. Yue, *Mater. Horiz.* **2022**, *9*, 973.
[48] C. B. Nielsen, A. Giovannitti, D.-T. Sbircea, E. Bandiello, M. R. Niazi, D. A. Hanifi, M. Sessolo, A. Amassian, G. G. Malliaras, J. Rivnay, I. McCulloch, *J. Am. Chem. Soc.* **2016**, *138*, 10252.
[49] S. Ma, J. Wang, W. Wu, Z. Wu, H. Zhang, R. Chen, B. Liu, K. Feng, H. Y. Woo, X. Guo, *Adv. Electron. Mater.* **2023**, *9*, 2300207.
[50] S. Deng, C. Dong, J. Liu, B. Meng, J. Hu, Y. Min, H. Tian, J. Liu, L. Wang, *Angew. Chem., Int. Ed.* **2023**, *62*, 202216049.
[51] H. Wang, J. Huang, M. A. Uddin, B. Liu, P. Chen, S. Shi, Y. Tang, G. Xing, S. Zhang, H. Y. Woo, H. Guo, X. Guo, *ACS Appl. Mater. Interfaces* **2019**, *11*, 10089.
[52] Y. Gao, Y. Deng, H. Tian, J. Zhang, D. Yan, Y. Geng, F. Wang, *Adv. Mater.* **2017**, *29*, 1606217.
[53] K. Guo, J. Bai, Y. Jiang, Z. Wang, Y. Sui, Y. Deng, Y. Han, H. Tian, Y. Geng, *Adv. Funct. Mater.* **2018**, *28*, 1801097.
[54] C. Zhang, W. L. Tan, Z. Liu, Q. He, Y. Li, J. Ma, A. S. R. Chesman, Y. Han, C. R. McNeill, M. Heeney, Z. Fei, *Macromolecules* **2022**, *55*, 4429.

[55] M. Moser, A. Savva, K. Thorley, B. D. Paulsen, T. C. Hidalgo, D. Ohayon, H. Chen, A. Giovannitti, A. Marks, N. Gasparini, A. Wadsworth, J. Rivnay, S. Inal, I. McCulloch, *Angew. Chem., Int. Ed.* **2021**, *60*, 7777.
[56] Y. Lei, P. Li, Y. Zheng, T. Lei, *Mater. Chem. Front.* **2024**, *8*, 133.
[57] R. Noriega, J. Rivnay, K. Vandewal, F. P. V. Koch, N. Stingelin, P. Smith, M. F. Toney, A. Salleo, *Nat. Mater.* **2013**, *12*, 1038.
[58] R. Steyrleuthner, Y. Zhang, L. Zhang, F. Kraffert, B. P. Cherniawski, R. Bittl, A. L. Briseno, J.-L. Bredas, J. Behrends, *Phys. Chem. Chem. Phys.* **2017**, *19*, 3627.
[59] S. N. Afraj, C.-C. Lin, A. Velusamy, C.-H. Cho, H.-Y. Liu, J. Chen, G.-H. Lee, J.-C. Fu, J.-S. Ni, S.-H. Tung, S. Yau, C.-L. Liu, M.-C. Chen, A. Facchetti, *Adv. Funct. Mater.* **2022**, *32*, 2200880.
[60] A. Velusamy, Y.-Y. Chen, M.-H. Lin, S. N. Afraj, J.-H. Liu, M.-C. Chen, C.-L. Liu, *Adv. Sci.* **2024**, *11*, 2305361.
[61] I. Zozoulenko, A. Singh, S. K. Singh, V. Gueskine, X. Crispin, M. Berggren, *ACS Appl. Polym. Mater.* **2019**, *1*, 83.
[62] L. Q. Flagg, C. G. Bischak, J. W. Onorato, R. B. Rashid, C. K. Luscombe, D. S. Ginger, *J. Am. Chem. Soc.* **2019**, *141*, 4345.
[63] D. Ohayon, V. Druet, S. Inal, *Chem. Soc. Rev.* **2023**, *52*, 1001.
[64] K. Feng, W. Shan, S. Ma, Z. Wu, J. Chen, H. Guo, B. Liu, J. Wang, B. Li, H. Y. Woo, S. Fabiano, W. Huang, X. Guo, *Angew. Chem., Int. Ed.* **2021**, *60*, 24198.
[65] K. Feng, W. Shan, J. Wang, J.-W. Lee, W. Yang, W. Wu, Y. Wang, B. J. Kim, X. Guo, H. Guo, *Adv. Mater.* **2022**, *34*, 2201340.
[66] A. Giovannitti, I. P. Maria, D. Hanifi, M. J. Donahue, D. Bryant, K. J. Barth, B. E. Makdah, A. Savva, D. Moia, M. Zetek, P. R. F. Barnes, O. G. Reid, S. Inal, G. Rumbles, G. G. Malliaras, J. Nelson, J. Rivnay, I. McCulloch, *Chem. Mater.* **2018**, *30*, 2945.
[67] M. Moser, L. R. Savagian, A. Savva, M. Matta, J. F. Ponder Jr, T. C. Hidalgo, D. Ohayon, R. Hallani, M. Reisjalali, A. Troisi, A. Wadsworth, J. R. Reynolds, S. Inal, I. McCulloch, *Chem. Mater.* **2020**, *32*, 6618.
[68] A. Giovannitti, K. J. Thorley, C. B. Nielsen, J. Li, M. J. Donahue, G. G. Malliaras, J. Rivnay, I. McCulloch, *Adv. Funct. Mater.* **2018**, *28*, 1706325.
[69] R. K. Hallani, K. J. Thorley, Y. Mei, S. R. Parkin, O. D. Jurchescu, J. E. Anthony, *Adv. Funct. Mater.* **2016**, *26*, 2341.